Highly Potent Inhibitors of Quorum Sensing in *Staphylococcus aureus* Revealed Through a Systematic Synthetic Study of the Group-III Autoinducing Peptide

Yftah Tal-Gan,[†,§] Danielle M. Stacy,[†,§] Mary K. Foegen,[‡] David W. Koenig,[‡] and Helen E. Blackwell*,[†]

[†]Department of Chemistry, University of Wisconsin−Madison, 1101 University Avenue, Madison, Wisconsin 53706, United States
[‡]Kimberly-Clark Corporation, 2100 Winchester Road, Neenah, Wisconsin 54956, United States

S Supporting Information

ABSTRACT: Methods to intercept bacterial quorum sensing (QS) have attracted significant attention as potential anti-infective therapies. *Staphylococcus aureus* is a major human pathogen that utilizes autoinducing peptide (AIP) signals to mediate QS and thereby regulate virulence. *S. aureus* strains are categorized into four groups (I−IV) according to their AIP signal and cognate extracellular receptor, AgrC. Each group is associated with a certain disease profile, and *S. aureus* group-III strains are responsible for toxic shock syndrome and have been underestimated in other infections to date. A limited set of non-native AIP analogs have been shown to inhibit AgrC receptors; such compounds represent promising tools to study QS pathways in *S. aureus*. We seek to expand this set of chemical probes and report herein the first design, synthesis, and biological testing of AIP-III mimetics. A set of non-native peptides was identified that can inhibit all four of the AgrC receptors (I−IV) with picomolar IC$_{50}$ values in reporter strains. These analogs also blocked hemolysis by wild-type *S. aureus* group I−IV strains—a virulence trait under the control of QS—at picomolar concentrations. Moreover, four of the lead AgrC inhibitors were capable of attenuating the production of toxic shock syndrome toxin-1 (also under the control of QS) by over 80% at nanomolar concentrations in a wild-type *S. aureus* group-III strain. These peptides represent, to our knowledge, the most potent synthetic inhibitors of QS in *S. aureus* known, and constitute new and readily accessible chemical tools for the study of the AgrC system and virulence in this deadly pathogen.
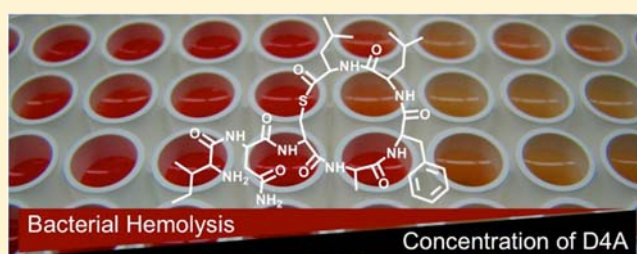
INTRODUCTION

Many bacteria utilize chemical signals to assess their local population densities in a process termed quorum sensing (QS).[1−3] This intercellular signaling process effectively allows bacteria to "count" themselves and behave as a multicellular group at high cell number. While the specifics may vary between species, QS circuits share general organizing principles: bacteria produce, secrete, and detect signal molecules referred to as autoinducers. At high population densities in a given environment, the autoinducers will reach a sufficiently high concentration to bind and activate their cognate receptors. Signal:receptor binding then alters the expression of genes involved in bacterial group behaviors, such as swarming, sporulation, bioluminescence, conjugation, biofilm formation, and virulence factor production.[4−6] These phenotypes can have widespread and sometimes devastating effects on human health, agriculture, and the environment.[7,8] For example, many pathogenic bacteria utilize QS to launch synchronized attacks on their hosts only after they have achieved a high cell density, thereby overwhelming the host's defense mechanisms.[9−11] As several prevalent human pathogens (e.g., *Staphylococcus aureus*, *Pseudomonas aeruginosa*, and *Vibrio cholerae*) use QS to control virulence, QS has received

considerable recent attention as a novel anti-infective target.[12,13] In turn, the dependence of bacteria on small molecule and peptidic signals for QS has ignited interest in the development of non-native ligands capable of blocking QS pathways.[14] In contrast to antibiotics, which target bacterial pathways that are essential for survival,[15,16] QS antagonists could provide an alternative anti-infective therapy[17,18] that does not place selective pressure on the bacterial population to develop resistance.[19] This is especially important in the case of *S. aureus*, which rapidly develops resistance to antibiotics, including to the once last-resort antibiotic vancomycin.[20]

S. aureus is a Gram-positive bacterium that uses QS to establish both acute and chronic infections.[21,22] This pathogen produces an arsenal of virulence factors, including tissue-degrading enzymes, immune evasion factors, and pore-forming toxins (hemolysins), all of which are regulated by its accessory gene regulator (agr) QS system.[23−25] The agr system is comprised of four components, termed AgrA−D (illustrated in Figure 1A), and is centered on the autoinducing peptide (AIP) QS signal. AgrB is an integral membrane endopeptidase that
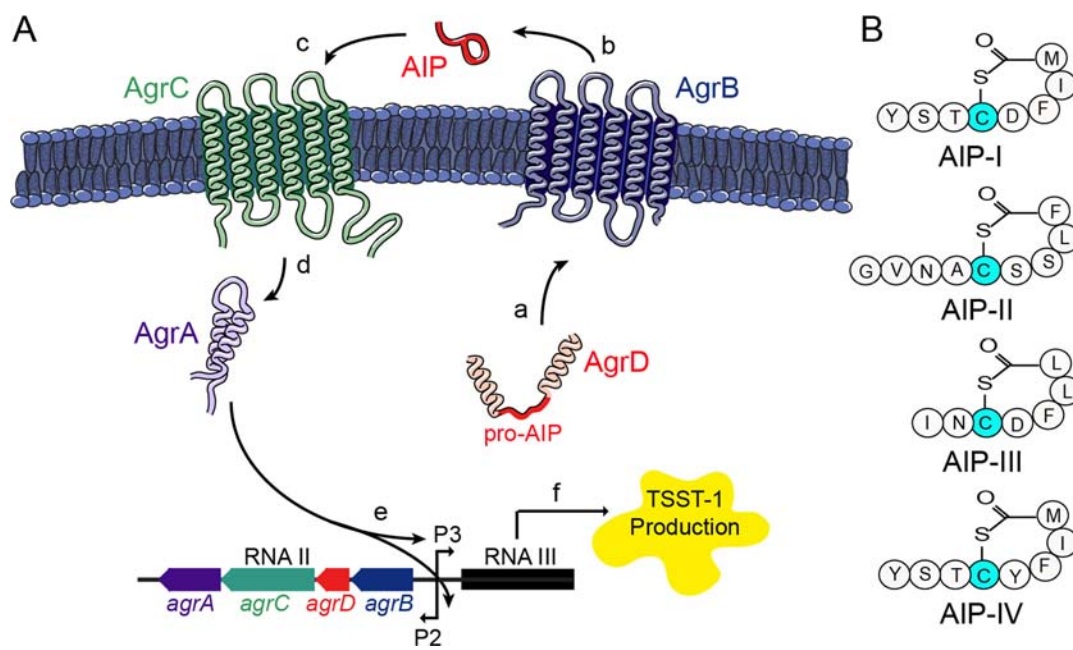
Figure 1. Schematic of the agr quorum sensing circuit in *S. aureus*. (A) (a) The precursor peptide AgrD is processed by AgrB. (b) The mature AIP signal is secreted across the cell membrane. (c) AIP binds the extracellular domain of AgrC. (d) The histidine kinase domain of AgrC phosphorylates AgrA. (e) AgrA binds the P2 and P3 promoters to autoactivate the agr system and upregulate RNAIII transcription. (f) In certain group-III *S. aureus* strains, RNAIII promotes the production of TSST-1. (B) Structures and sequences of the four AIP signals (I–IV) corresponding to the four *S. aureus* groups (I–IV). Letters represent amino acid codes.

converts the precursor of the AIP signal, AgrD, to the mature AIP. This conversion involves cyclization of AgrD via a cysteine sulfhydryl group and its C-terminus to form the AIP as a 16-atom thiolactone macrocycle with an N-terminal exocyclic tail (Figure 1B). AgrB is also involved in the secretion of AIP across the cell membrane. Once a threshold extracellular concentration of AIP is reached, the AIP ligand binds to its target receptor AgrC, a transmembrane histidine kinase. The AIP:AgrC complex acts to phosphorylate the intracellular response regulator, AgrA. Phosporylated AgrA then binds to the P2 and P3 promoters to autoinduce the agr system and upregulate RNAIII transcription, respectively.[26] RNAIII thus represents the main effector of the agr system and regulates the production of many virulence factors and surface proteins associated with biofilm production.[27]

There is a hypervariable region within the *S. aureus* agr operon that has led to the classification of four agr specificity groups of *S. aureus* (I–IV) with distinct AIP and AgrC sequences.[28–30] The structures of the four AIP signals (I–IV) are shown in Figure 1B; all have a conserved 16-atom thiolactone macrocycle, and AIPs-I and -IV share a nearly identical primary sequence, while AIP-II and AIP-III have more dissimilar primary sequences. The four different *S. aureus* agr groups have been correlated with specific disease types: group-I and -II are associated with the majority of invasive infections,[31–33] while group-IV is considered rare and limited to exfoliative toxin-related syndromes.[31] At first, group-III *S. aureus* was also considered rare. However, recent studies have revealed that the prevalence of this group has been underestimated in infections, and in fact, it is the most abundant group in nasal carriage cases and is predominately responsible for toxic shock syndrome (TSS) in humans.[31,32] Toxic shock syndrome toxin-1 (TSST-1) is the causative agent in all cases of menstrual TSS and most cases of nonmenstrual TSS.[31,34] Notably, TSST-1 production is directly regulated by the agr-III

QS system (Figure 1A).[23,34,35] As such, methods to inhibit the agr-III system in *S. aureus* could provide new insights into and therapeutic strategies for this deadly disease.

QS is dependent on autoinducer:receptor binding, and the development of chemical agents capable of blocking this binding event has been a focus of considerable research over the past ∼20 years.[36–40] Such abiotic agents represent promising tools to further elucidate the role of QS pathways in bacterial virulence and other group behaviors.[12,14,41–43] Our laboratory has been actively engaged in the development of small molecule QS modulators, largely in Gram-negative bacteria that use LuxR-type receptors for QS.[37,44–48] The development of small molecule tools to probe AgrC signaling in *S. aureus* has proceeded more slowly in the research community, however.[49] We note that Janda and co-workers have reported a complementary, macromolecular strategy based on antibodies that sequester the AIP ligand away from AgrC and effectively "quench" QS in group-IV *S. aureus*.[50,51] McCormick and co-workers have also shown that naturally occurring cyclic dipeptides produced by *Lactobacillus reuteri* ((cyclo-(Tyr-Pro) and cyclo-(Phe-Pro)) can modulate the agr system in *S. aureus* (albeit at mid- to high micromolar concentrations), suggesting an interesting possibility for interspecies signaling between Gram-positive bacteria using small molecules.[34] Nevertheless, new strategies are needed to expand the chemical arsenal active against the agr QS system.

Early studies of the AgrC receptors revealed that each of the four native AIPs were capable of cross-inhibiting the other three, noncognate receptors.[28,52–54] This activity has been suggested to provide each group some competitive advantage when establishing an infection and could explain in part the predominance of a single *S. aureus* group in many infection types (see above).[28,55] In terms of the design of peptidic non-native AgrC modulators, AIP-I and -II have received the most scrutiny so far.[29,52,53,56–59] Studies by Muir, Novick, Williams,

and co-workers closely examined the SAR of AIPs-I and -II[60−62] and provided the first non-native mimetics of these peptides that were capable of inhibiting both their cognate and noncognate AgrC receptors in *S. aureus*. This group delineated two key components of AIP:AgrC interactions: (1) initial recognition of the AIP by an AgrC receptor, and (2) the subsequent induction of allosteric changes within the AgrC receptor that drives activation. In general, the AIP macrocycle was found to be responsible for initial receptor recognition/ binding, and the AIP exocyclic tail then engaged in interactions that resulted in receptor activation.[62] For instance, the acyclic native AIP-II was completely inactive, indicating that an intact macrocyclic core was essential for activity.[52] Removal of the exocyclic tail converted the native AIPs-I and -II into self-inhibitors, suggesting that these truncated peptides could bind yet could not activate their cognate AgrC receptors. Likewise, alterations to the native AIP exocyclic tails did not significantly affect their cross-inhibitory activities against noncognate AgrCs, which implied that these activities also result from macro-cycle:receptor binding. Within the AIP-I and -II macrocycles, the hydrophobic residues at the C-termini (residues 6−8 for AIP-I and residues 8 and 9 for AIP-II; Figure 1B) were found to be critical for both cognate and noncognate AgrC recognition/ binding.[29,52,56] By combining these observations, Muir and co-workers identified several potent and global inhibitors of all four AgrC receptors (I−IV).[56] Their most active inhibitor was a truncated version of AIP-I that lacked an exocyclic tail and had an aspartic acid (D) to alanine (A) mutation in the macrocyclic core (tAIP-I D2A, shown in Figure 2).

Many questions remain about the mode of action of native AIPs and the peptide-based AgrC modulators developed so far,
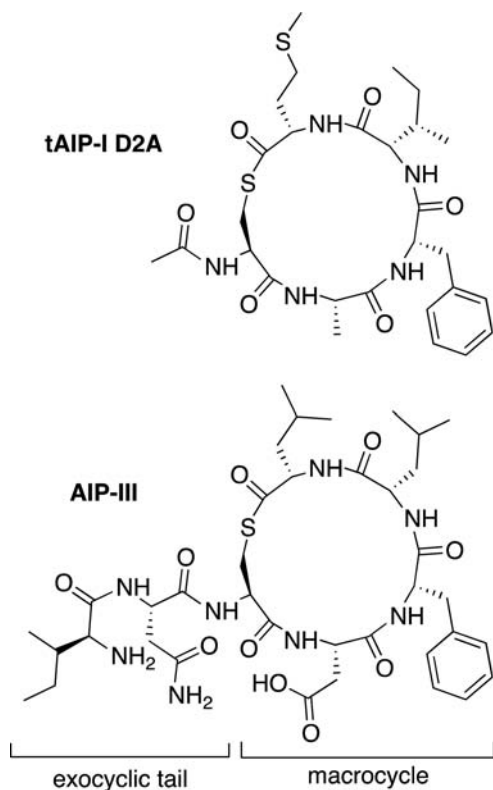
and these prior studies provide a foundation on which to expand the current set of non-native AgrC agonists and antagonists.[63] In the present study, we focused on AIP-III (Figure 2) as the SARs that dictate its activity remain largely unknown, and mimetics thereof are yet to be reported. The prevalence of group-III *S. aureus* infections in human TSS (*vide supra*) provides additional motivation for the development of such molecules. Herein, we report the design, synthesis, and systematic biological testing of a series of first- and second-generation AIP-III mimetics. Evaluation of these mutant peptides for their ability to attenuate each of the four AgrC receptors (I−IV) revealed three key residues (i.e., Ile1, Asn2, and Asp4) that can be modified in AIP-III to produce potent AgrC inhibitors. Notably, a set of AIP-III analogs was identified that can inhibit all four of the AgrC receptors with picomolar IC_{50} values in cell-based reporter gene assays. All of these analogs also blocked hemolysis by wild-type *S. aureus*—a virulence phenotype under the control of QS—at picomolar levels. Moreover, the lead compounds were capable of reducing TSST-1 production levels in a wild-type *S. aureus* group-III strain by over 80% at low nanomolar concentrations. The results of this study are significant, as these peptides represent, to our knowledge, the most potent *S. aureus* QS inhibitors to be reported and suggest that, relative to the other AIPs, AIP-III provides a superior scaffold for the development of peptide-based AgrC inhibitors. More broadly, these new peptides represent readily accessible chemical tools for the study of the agr QS system and virulence in this deadly pathogen and provide support for the potential development of QS inhibitors as anti-infective agents.

■ EXPERIMENTAL SECTION

Chemical Reagents and Instrumentation. All chemical reagents were purchased from commercial sources (Alfa-Aesar, Sigma-Aldrich, and Acros) and used without further purification. Solvents were purchased from commercial sources (Sigma-Aldrich and J.T. Baker) and used as obtained, with the exception of anhydrous dichloro-methane (CH_2Cl_2), which was stored over molecular sieves. Water (18 MΩ) was purified using a Millipore Analyzer Feed System. Solid-phase resin was purchased from Chem-Impex International. Cyclic dipeptide (cyclo-(Tyr-Pro) and cyclo-(Phe-Pro)) controls were synthesized according to our previously reported method.[64]

Reversed-phase high-performance liquid chromatography (RP-HPLC) was performed using a Shimadzu system equipped with an SCL-10Avp controller, an LC-10AT pump, an FCV-10ALvp solvent mixer, and an SPD-10MAvp UV−vis diode array detector. Full details of the HPLC columns and conditions used in this study are provided in the Supporting Information. Matrix-assisted laser desorption ionization time-of-flight mass spectrometry (MALDI-TOF MS) data were obtained on a Bruker RELEX II spectrometer equipped with a 337 nm laser and a reflectron. In positive ion mode, the acceleration voltage was 25 kV. Exact mass (EM) data were obtained on a Waters (Micromass) LCT electrospray ionization TOF spectrometer. The samples were sprayed with a sample cone voltage of 20 V.

Peptide Synthesis. Table 1 lists the peptides synthesized in this study. Linear peptides were synthesized on Boc-protected, amino acid preloaded 4-hydroxymethyl-phenylacetamidomethyl (PAM) resin (0.6−0.8 mmol/g) using standard solid-phase synthesis protocols; see Supporting Information for full details of peptide synthesis, cleavage, HPLC purification, and MS analyses.

Representative Peptide Macrocyclization Protocol. Purified peptide thioester was dissolved in a 60% guanidinium chloride (6 M solution in 0.1 M phosphate buffer):40% ACN solution to a final concentration ranging from 100 μM to 2 mM. The pH of the solution was then adjusted to 6.8. The peptide was gently agitated using a multipurpose rotator at 50 °C, and cyclization was monitored by

Figure 2. Structures of a known global AgrC inhibitor tAIP-I D2A (top) and AIP-III (bottom). The two main structural elements of the AIP signals (exocyclic tail and macrocycle core) are highlighted.

Table 1. Structures of the Peptides Synthesized in This Study[a]

peptide name	sequence	peptide name	sequence
AIP-I[b]	Y−S-T-(C-D-F-I-M)	AIP-III[b]	I-N-(C-D-F-L-L)
AIP-II[b]	G-V-N-A-(C-S-S-L-F)	AIP-IV[b]	Y-S-T-(C-Y-F-I-M)
tAIP-I D2A[b]	Ac-(C-A-F-I-M)		
first generation analogs		*second generation analogs*	
AIP-III D-I1	DI-N-(C-D-F-L-L)	AIP-III I1A/N2A	A-A-(C-D-F-L-L)
AIP-III D-N2	I-DN-(C-D-F-L-L)	AIP-III I1A/D4A	A-N-(C-A-F-L-L)
AIP-III D-C3	I-N-(DC-D-F-L-L)	AIP-III N2A/D4A	I-A-(C-A-F-L-L)
AIP-III D-D4	I-N-(C-DD-F-L-L)	AIP-III I1A/N2A/D4A	A-A-(C-A-F-L-L)
AIP-III D-F5	I-N-(C-D-DF-L-L)	tAIP-III	Ac-(C-D-F-L-L)
AIP-III D-L6	I-N-(C-D-F-DL-L)	tAIP-III D2A	Ac-(C-A-F-L-L)
AIP-III D-L7	I-N-(C-D-F-L-DL)	tAIP-III D2A/F3Y	Ac-(C-A-Y-L-L)
AIP-III I1A	A-N-(C-D-F-L-L)	tAIP-III D2A/F3W	Ac-(C-A-W-L-L)
AIP-III N2A	I-A-(C-D-F-L-L)	Ac-AIP-III	Ac-I-N-(C-D-F-L-L)
AIP-III D4A	I-N-(C-A-F-L-L)	G-AIP-III	G-I-N-(C-D-F-L-L)
AIP-III F5A	I-N-(C-D-A-L-L)	A-AIP-III	A-I-N-(C-D-F-L-L)
AIP-III L6A	I-N-(C-D-F-A-L)	Y-AIP-III	Y-I-N-(C-D-F-L-L)
AIP-III L7A	I-N-(C-D-F-L-A)		

[a]See Table S-1 for MS and HPLC characterization data. [b]Represents control peptides.

analytical RP-HPLC. Upon completion, cyclic peptide was purified by semipreparative RP-HPLC and lyophilized. The resulting white powder was dissolved in a small portion of 1 M hydrochloric acid (~400 μL) and lyophilized prior to bioanalysis.

Biological Reagents and Strain Information. All standard biological reagents were purchased from Sigma-Aldrich and used according to enclosed instructions. Suspended rabbit blood cells (10%, washed and pooled) were purchased from Lampire Biological Laboratories and stored at 4 °C until use in the hemolysis assay. Reagents for the TSST-1 enzyme-linked immunosorbent assay (ELISA) were purchased from Toxin Technology, Inc. Tryptic soy broth (TSB) and brain heart infusion (BHI) were prepared as instructed with pH = 7.35.

The bacterial strains used in this study are listed in Table 2. Bacterial cultures were grown in a standard laboratory incubator at 37

Table 2. S. aureus Strains Used in This Study Listed According to Group

assay type	strain	ref.
Fluorescence		
group-I	AH1677	51
group-II	AH430	51, 65
group-III	AH1747	51
group-IV	AH1872	51
Hemolysis and TSST-1		
group-I	RN6390B	27
group-II	RN6923	28
group-III	MN8	66
group-IV	RN4850	30

°C with shaking (200 rpm) unless noted otherwise. The bacterial dilutions and incubation periods were chosen in each assay to provide the greatest dynamic range between positive and negative controls for each bacterial strain. Absorbance and fluorescence measurements were obtained using a Biotek Synergy 2 microplate reader using Gen5 data analysis software. All biological assays were performed in triplicate. IC$_{50}$ values were calculated using GraphPad Prism software (v. 4.0) using a sigmoidal curve fit.

Compound Handling Protocol. Stock solutions of synthetic AIP analogs (1 mM) or cyclic dipeptides (10 mM) were prepared in DMSO and stored at 4 °C in sealed vials. The amount of DMSO used in biological assays did not exceed 2% (v/v). Black or clear polystyrene 96-well microtiter plates (Costar) were used for bacteriological assays.

Clear polystyrene 96-well EIA/RIA high-binding microtiter plates (Costar) were used in the TSST-1 ELISA.

Reporter Gene Assay Protocol. Peptide stock solutions were diluted with DMSO in serial dilutions (either 1:3, 1:5, or 1:10), and 2 μL of the diluted solution was added to each of the wells in a black 96-well microtiter plate. An overnight culture of *S. aureus* gfp strain was diluted 1:50 with fresh TSB (pH 7.35). A 198 μL portion of diluted culture was added to each well of the microtiter plate containing peptide. Plates were incubated at 37 °C for 24 h. Fluorescence (EX 500 nm/EM 540 nm) and OD$_{600}$ of each well were then recorded using a plate reader, and IC$_{50}$ values were calculated.

For the competition assays, 2 μL of AIP-III D4A stock solution was added to wells in a black 96-well microtiter plate to final concentrations of 2 nM (group-I and -II strains) or 0.3 nM (group-III and -IV strains). Native AIP (I−IV) stock solutions were diluted with DMSO in serial dilutions (1:3 dilutions) and added to the wells containing AIP-III D4A. The fluorescence assay was performed as described above in the four respective *S. aureus* reporter strains.

Hemolysis Assay Protocol. Peptide stock solutions were diluted with DMSO in serial dilutions (either 1:3, 1:5, or 1:10), and 2 μL of the diluted peptide solution was added to each of the wells in a clear 96-well microtiter plate. An overnight culture of *S. aureus* wild-type strain was diluted (1:10, 1:25, or 1:100, assay conditions dependent on strain; see Table S-2 for additional detail) with fresh TSB. A 198 μL portion of the diluted culture was added to each well of the microtiter plate containing peptides. Plates were incubated statically at 37 °C for 6−8 h. The cultures were then assayed for hemolytic activity. Suspended rabbit red blood cells (1 mL) were centrifuged (2000 rpm, 2 min, 25 °C, 450 g), the supernatant was removed, and the cells were resuspended in saline phosphate buffer (PBS, pH = 7.35, 1 mL). After the OD$_{600}$ of each well of the 96-well microtiter plate was recorded, a 13 μL portion of the suspended red blood cells was added to each well. After 15−25 min (see Table S-2) of static incubation at 37 °C, the microtiter plates were centrifuged to pellet the cells (4 min, 25 °C, 450 g). A 150 μL portion of supernatant from each well of culture was transferred to a fresh 96-well microtiter plate. Absorbance at 420 nm was measured for each well using a plate reader, and IC$_{50}$ values were calculated.

TSST-1 ELISA Protocol. The TSST-1 ELISA protocol was based in part on the procedure supplied by the toxin producer (Toxin Technologies, Inc.) with some modifications. Peptide stock solutions (AIP-III analog or cyclic dipeptide control) were diluted with DMSO to the desired concentration, and 20 μL of the diluted solutions was added to 15 mL Falcon tubes. An overnight culture of *S. aureus* MN8 was diluted 1:100 with fresh BHI, and a 1 mL portion of diluted

culture was added to each Falcon tube containing peptide. The cultures were incubated at 37 °C for 24 h. Simultaneously, rabbit polyclonal anti-TSST-1 IgG (100 μL, 10 μg/mL in coating buffer (0.01 M sodium carbonate, pH 9.6)) was added to a 96-well ELISA plate and incubated with shaking (200 rpm) in a humid chamber (i.e., a sealed plastic box containing several water-soaked paper towels) at 37 °C for 18 h. The ELISA plate was then washed 3× (300 μL each) with PBS solution containing 0.05% Tween-20 (PBS-Tween). To block the plate, bovine serum albumin (BSA, 1% in PBS-Tween, 100 μL) was added to each well and incubated for 15 min at rt, after which it was washed 3× again with PBS-Tween (300 μL each).

The bacterial cultures were centrifuged to pellet the cells (10 min, 25 °C, 450 g), and the supernatants were sterile filtered. The supernatants were diluted 1:10 in normal rabbit serum (NRS, 1% in PBS-Tween) and incubated for 15 min at rt. The incubated solutions were further diluted using PBS-Tween to a total dilution of 1:100 to 1:2000. The diluted supernatant samples (100 μL) and TSST-1 standards with known concentrations (ranging from 10 ng/mL to 0.32 ng/mL, 100 μL) were added to the ELISA plate and incubated with shaking (200 rpm) in a humid chamber at 37 °C for 2 h. After incubation, the plate was washed 3× with PBS-Tween (300 μL each), and anti-TSST-1 IgG horseradish peroxidase conjugate (100 μL, 3.33 μg/mL) was added and incubated with shaking (200 rpm) in a humid chamber at 37 °C for 1 h. The plate was washed 5× with PBS-Tween (300 μL each), after which 2,2′-azinobis(3-ethylbenzthiazoline-sulfonic acid) (ABTS solution, 100 μL) was added and incubated at rt for 15 min. Absorbance at 405 nm was measured using a plate reader, and a TSST-1 standard curve was constructed for each assay plate using the data for the TSST-1 reference standards (the R^2 of linear regression analysis for these data was ≥0.99). The TSST-1 concentration in the test samples was then determined from the regression equation and presented as a percentage of the TSST-1 concentration in the untreated cultures.

■ RESULTS AND DISCUSSION

Design of First-Generation AIP-III Analogs. We initiated our research by independently evaluating each residue of AIP-III through systematic alanine and D-amino acid point mutations. This initial set of 13 peptides was designed to identify key residues and stereocenters for AIP-III:AgrC interactions. Six of the seven residues could be modified in the alanine scan (Cys3 had to be maintained for thiolactone formation), while all seven residues were evaluated in the D-amino acid scan. The 13 AIP-III analogs were generated by solid-phase synthesis (Table 1), as detailed below.

Synthesis of AIPs and Analogs. Two solid-phase synthesis approaches have been implemented in the past to construct native AIPs and their analogs. The first approach utilizes chemoselective cleavage of the linear, protected peptide from the solid support with concomitant unmasking of the cysteine sulfhydryl group. The protected peptide can then be macrocyclized via a carbodiimide coupling and subsequently deprotected.[29,57,67] This approach, however, is limited in part by the poor solubilities of the protected peptides and by low macrocyclization efficiencies due to the steric bulk of the protecting groups. The second synthetic approach addresses these challenges by incorporating an initial global deprotection step prior to a solution phase, chemoselective thiol-thioester exchange to form the macrocyclic products.[52,56,58] This latter approach is generally more efficient and has the potential for even further improvement; we therefore selected this strategy to synthesize our AIP-III analogs. First, we utilized standard Fmoc/tBu solid-phase peptide synthesis methods to generate the linear peptides on 4-hydroxymethyl-phenylacetamido-methyl (PAM) polystyrene resin (Scheme 1; see Experimental Section). Cleavage and global deprotection according to the

Scheme 1. Solid-Phase Synthetic Route to AIPs and Analogs[a]
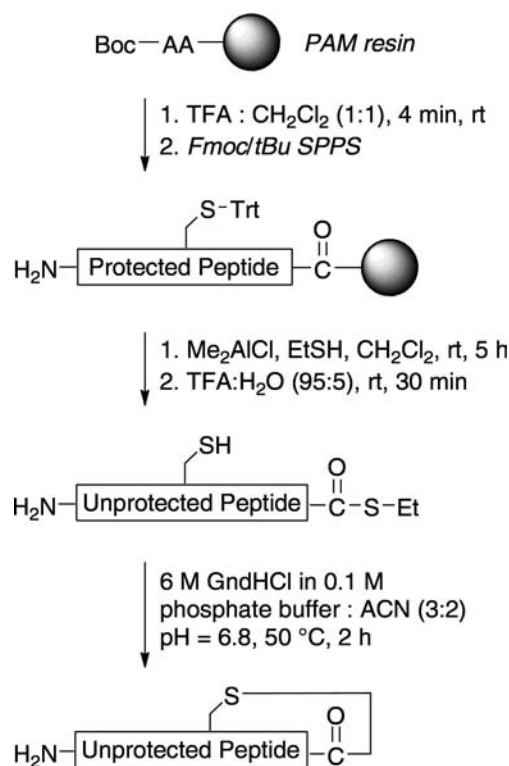
[a]See Experimental Section for further details. TFA = trifluoroacetic acid; SPPS = solid-phase peptide synthesis; GndHCl = guanidinium chloride.

method of Hilvert and co-workers gave the linear peptide thioesters,[68,69] which were then purified to homogeneity by semipreparative RP-HPLC and isolated in acceptable yields (25−50%).

We next explored intramolecular thiol-thioester exchange reactions in a range of buffers to effect macrocyclization of the linear peptides (Scheme 1). However, the previously reported cyclization buffers and conditions proved ineffective in our hands, even after 24 h.[56,58] We therefore undertook optimization studies to develop our own macrocyclization conditions and found that performing the reaction in 6 M guanidinium chloride in 0.1 M phosphate buffer and ACN (3:2) at a pH = 6.8 gave quantitative macrocyclization within 24 h at room temperature. Elevating the temperature to 50 °C reduced reaction times to <2 h (see Figure S-1 for HPLC analyses of macrocyclization reactions). We therefore used these conditions to effect macrocyclization of all the AIP analogs prepared in this study (Table 1; see Supporting Information for full characterization details). We also used this synthesis protocol to generate the four native AIPs I−IV and the known global AgrC inhibitor, tAIP-I D2A (Figure 2), for use as key controls in our biological experiments (see below). Overall, this synthetic route to AIPs represents an improvement over previously reported methods[52,56,58] and will facilitate research in this general area. Further, the thiol-thioester exchange reaction conditions could also prove useful in other contexts, for example, in the total synthesis of proteins using native chemical ligation.[70]

S. aureus Reporter Gene Assays. We next tested the ability of the 13 alanine and D-amino acid AIP-III mutants to

Table 3. IC$_{50}$ Values of the Alanine and D-Amino Acid Scan Analogs of AIP-III Against AgrC I–IV Determined Using *S. aureus* Fluorescence Reporter Strains[a]

peptide name	sequence	AgrC-I IC$_{50}$ (nM)[b]	AgrC-II IC$_{50}$ (nM)[b]	AgrC-III IC$_{50}$ (nM)[b]	AgrC-IV IC$_{50}$ (nM)[b]
AIP-III D-I1	DI-N-(C-D-F-L-L)	8.42	16.4	78.3	77.7
AIP-III D-N2	I-DN-(C-D-F-L-L)	2.15	2.45	17.8	6.23
AIP-III D-C3	I-N-(DC-D-F-L-L)	>200	>200	>200	>200
AIP-III D-D4	I-N-(C-DD-F-L-L)	138	24.5	>200	29.2
AIP-III D-F5	I-N-(C-D-DF-L-L)	>200	>200[c,d]	>200	174
AIP-III D-L6	I-N-(C-D-F-DL-L)	>200	–[e]	>200	>200
AIP-III D-L7	I-N-(C-D-F-L-DL)	12.0	5.36	–[e]	10.5
AIP-III I1A	A-N-(C-D-F-L-L)	17.9	4.26	194	7.85
AIP-III N2A	I-A-(C-D-F-L-L)	3.60	0.732	–[c,d]	3.53
AIP-III D4A	I-N-(C-A-F-L-L)	0.485	0.429	0.0506	0.0349
AIP-III F5A	I-N-(C-D-A-L-L)	>200	>200[c]	>200	118
AIP-III L6A	I-N-(C-D-F-A-L)	>200	>200	>200	>200
AIP-III L7A	I-N-(C-D-F-L-A)	>200	>200	>200	>200
AIP-I[f]	Y-S-T-(C-D-F-I-M)	–[e]	8.00	0.522	–[c,d]
AIP-II[f]	G-V-N-A-(C-S-S-L-F)	1.62	–[e]	0.532	0.396
AIP-III[f]	I-N-(C-D-F-L-L)	5.05	5.63	–[e]	8.53
AIP-IV[f]	Y-S-T-(C-Y-F-I-M)	–[c,d]	0.373	0.460	–[e]
tAIP-I D2A[f]	Ac-(C-A-F-I-M)	3.06	10.1	0.260	0.353
Cyclo(Tyr-Pro)[f]	(Y-P)	–[g]	–[g]	–[g]	–[g]
Cyclo(Phe-Pro)[f]	(F-P)	–[g]	–[g]	–[g]	–[g]

[a]See Experimental Section for details of reporter strains and methods. See Supporting Information for plots of antagonism dose response curves. All assays performed in triplicate. [b]IC$_{50}$ values determined by testing peptides over a range of concentrations (200 fM – 100 μM). See Figure 4 and Supporting Information for 95% confidence ranges. [c]Dose response curve did not reach 100% inhibition over the concentrations tested. [d]Inhibition dose response curve upturned at higher concentrations, potentially indicative of partial agonism (see text). [e]Dose response curve revealed agonism and no antagonism. [f]Control compound. [g]No activity at any concentration tested up to at least 100 μM. Higher concentrations could not be tested due to compound insolubility.

modulate the activity of the *S. aureus* AgrC I–IV receptors using fluorescence-based reporter gene assays (see Experimental Section for protocol). Each compound was tested in group I–IV methicillin-resistant *S. aureus* strains harboring P3-*gfp* reporter plasmids (listed in Table 2).[51,65] In these reporter plasmids, the agr P3 promoter, typically upstream of the main QS effector RNAIII (Figure 1A), is also upstream of *gfp*. Thus, when bacterial cell densities and AIP concentrations are high, the AIP:AgrC complex will phosphorylate AgrA, which will then bind P3 and transcribe *gfp* (in addition to typical upregulation of RNAIII). *GFP* fluorescence can then be quantified to determine the extent of AgrC activation, and in these wild-type strains (producing native levels of AIP) will be observable in the absence of an exogenous AgrC modulator. Compounds capable of reducing fluorescence levels (or increasing these levels over background), therefore, can be classified as AgrC inhibitors (or activators). We note that previous researchers have utilized a similar strategy to identify AgrC modulators in all four groups of *S. aureus* but used a group-I *agr*-null strain carrying a plasmid containing a P3-*blaZ* fusion (to confer β-lactamase activity in response to AgrC activation) and *agrCA* from groups-I, -II, -III, or -IV.[53,56] The gfp reporters utilized here allow for the analysis of analogs in all four wild-type strains producing native levels of AIPs I–IV. In order to have controls for comparison to our AIP-III analogs, we also evaluated the activities of the native AIPs I–IV, Muir's previously reported global AgrC inhibitor tAIP-I D2A,[56] and McCormick's previously reported cyclic dipeptide agr modulators ((cyclo-(Tyr-Pro) and cyclo-(Phe-Pro))[34] in each *S. aureus* gfp-reporter strain. The inhibitory trends for the native AIPs I–IV and tAIP-I D2A in each of the four AgrC receptors were comparable to previous reports using alternate *S. aureus*

AgrC I–IV reporter strains.[56] The two cyclic dipeptides were inactive in the four reporter strains over the concentration range tested (suggestive of IC$_{50}$ values much >100 μM), which was also congruent with the study of McCormick and co-workers.[34] Table 3 summarizes the activities of these control peptides and the first-generation AIP-III analogs against AgrCs I–IV in the gfp-reporter strains.

The reporter gene assay data revealed several interesting SAR trends for AIP-III. Moreover, a number of new, global AgrC inhibitors were uncovered with either comparable or more potent activities than the known inhibitor tAIP-I D2A (Table 3). As discussed above, there are two main components to AIP:AgrC interactions: (1) the initial recognition of the AIP by an AgrC receptor and (2) the resultant induction of allosteric changes within AgrC that drives activation. To explore these components for AIP-III, we examined two different SAR trends for the AIP-III analogs: (1) cross-inhibition of AgrC-I, -II, and -IV, and (2) activation of AgrC-III. Each is discussed in turn below.

Consistent with prior observations of other AIPs,[29,52,56] D-amino acid and alanine replacement of either of the exocyclic tail residues (Ile1 or Asp2) resulted in AIP-III analogs with similar cross-inhibitory activities to the parent AIP-III (Table 3, IC$_{50}$ values within error or <10-fold change). In addition, replacement of any one of the three hydrophobic endocyclic residues in AIP-III (Phe5, Leu6, or Leu7) with alanine resulted in a significant loss of inhibition in groups-I, -II, and -IV (>10-fold change relative to AIP-III). Replacement of Phe5 and Leu6 with their D-amino acid counterparts further demonstrated the stringent requirements of these two residues for inhibitory activity against AgrC receptors, as these mutants displayed a >20-fold loss in inhibition in almost every case. However, AIP-III

D-L7 displayed analogous inhibitory activities as the parent AIP-III in groups-I, -II and-IV (within error), suggesting that Leu7 may not enforce stereodefined interactions of AIP-III with these AgrC receptors. This observation is congruent with previous findings for AIP-I by Williams and co-workers.[29] We note two exceptions to these activity trends: replacing the endocyclic Phe5 or Leu6 with their D-isomers (in AIP-III D-F5 and AIP-III D-L6) neither maintained nor abolished inhibitory activity against one receptor, AgrC-II. These two analogs appeared to activate AgrC-II instead. The extent of this activation relative to native AIP could not be fully explored using the gfp-reporter assays in this study, however, as the native AIP signals are produced at normal background levels in these *S. aureus* reporter strains (see above). Alternate biological assays are required to study this phenomenon further and are ongoing.

The remaining two residues of AIP-III, Cys3 and Asp4, were found to contribute significantly to cross-receptor inhibition. The replacement of Cys3 with its D-isomer significantly reduced inhibition (>20-fold change relative to native AIP-III; Table 3). This reduction may be due to a conformational change caused by the reversed stereogenic center of cysteine, forcing a change in the orientation of the key hydrophobic residues in the macrocyclic backbone, thereby preventing AIP:AgrC recognition interactions. Additional studies are certainly needed to confirm this hypothesis. Replacement of Asp4 with its D-isomer also reduced inhibition against AgrC-I by 28-fold relative to AIP-III, yet reduced inhibitory activity to a lesser degree against AgrC-II and AgrC-IV (4- and 3-fold relative to AIP-III, respectively). This result suggests that the stereochemistry of Asp4 could reinforce optimal orientations of Phe5 and Leu6 for interactions with AgrC-I. Perhaps more notable, however, was that the replacement of Asp4 with alanine (AIP-III D4A) increased the inhibitory activity of AIP-III by at least 10-fold in each group, delivering a picomolar global AgrC inhibitor. Interestingly, AIP-III D4A contains the identical mutation as the previously reported global inhibitor generated from the AIP-I scaffold, tAIP-I D2A (residue numbering shifted (4→2) due to truncated structure), yet is a 5- to 24-fold more active inhibitor in each group (largest increase in potency against AgrC-II; see Table 3). AIP-III D4A represented not only the most active inhibitor identified in this first series of AIP-III derivatives, but also, to our knowledge, is the most potent AgrC inhibitor to be reported. The discovery of this lead compound from such a limited and structurally similar set of AIP-III derivatives provides strong support for further study of the AIP-III scaffold for the development of global AgrC inhibitors. A summary of the key SARs for cross-inhibition of AgrC-I, -II, and -IV by the AIP-III analogs is provided in Figure 3.

Analysis of the gfp screening data for the AIP-III analogs also provided valuable SAR trends for the activation of AgrC-III by AIP-III (Table 3). Although native AIP signals were present in these wild-type *S. aureus* reporter strains, we could infer AgrC-III inhibition as the competitive binding of the non-native AIP to AgrC-III and either lack of or partial AgrC-III activation. (We return to the reasoning behind this competitive mechanism argument below.) As expected, in view of previous studies of AIP-I and -II analogs,[29,52] the exocyclic residue Ile1 of AIP-III appeared to play an important role in AgrC-III activation. Replacing this residue with either alanine or D-Ile1 converted AIP-III into a weak antagonist (IC50 values = 194 or 78.3 nM, respectively). Converting the exocyclic residue Asn2 to its D-isomer yielded an even stronger AgrC-III antagonist
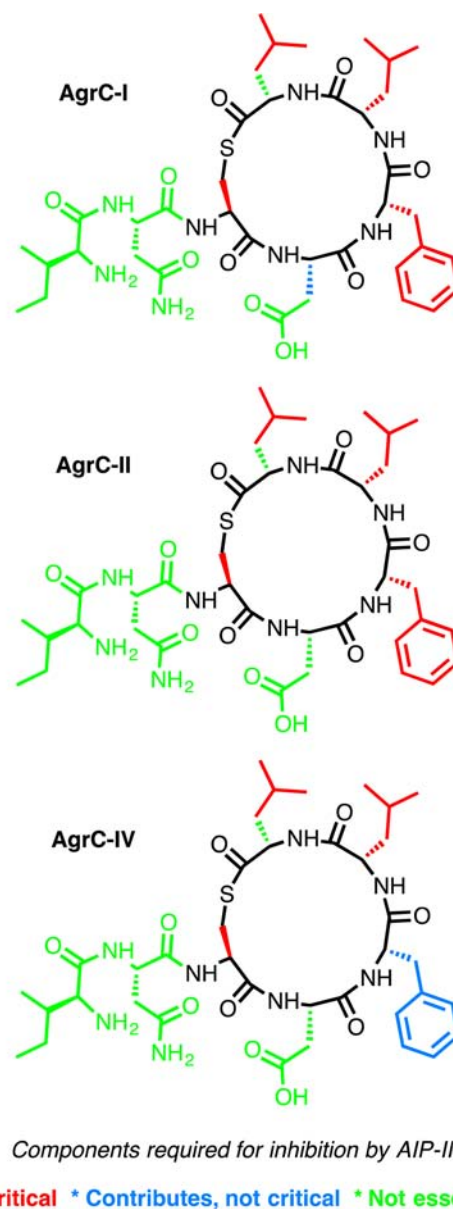

Components required for inhibition by AIP-III:

* Critical   * Contributes, not critical   * Not essential

Figure 3. Summary of key SAR trends for inhibition of AgrC-I, -II, and -IV by AIP-III analogs as revealed by the gfp-reporter assay data. See text.

(IC50 value = 17.8 nM). However, replacing Asn2 with alanine maintained agonistic activity, suggesting that the stereochemical presentation (and concomitant conformational constraints) of the peptide backbone may be more essential for AgrC-III activation relative to the composition of the Asn2 side chain.

Within the AIP-III macrocycle, the two hydrophobic residues Phe5 and Leu6 proved to be crucial for AgrC-III activation, as D-isomer or Ala replacements at either of these positions yielded weak AgrC-III inhibitors (IC50 values > 200 nM; Table 3). The AIP-III D-L7 mutant maintained the agonistic activity of the native AIP-III, while AIP-III L7A was also a weak inhibitor, similar to the AIP-III F5A and AIP-III L6A mutants. This disparate activity trend for the Leu7 mutants suggests that stereochemistry at this residue may not play as major of a role in AgrC-III activation relative to that for Phe5 and Leu6. We note that the activity profiles for these Phe5, Leu6, and Leu7 mutants in AgrC-III are largely consistent with the observed

Table 4. IC$_{50}$ Values of the Alanine and D-Amino Acid Scan Analogs of AIP-III for Inhibition of Hemolysis by Group-I—IV S. aureus Strains^a

peptide name	sequence	group-I IC$_{50}$ (nM)^b	group-II IC$_{50}$ (nM)^b	group-III IC$_{50}$ (nM)^b	group-IV IC$_{50}$ (nM)^b
AIP-III D-I1	DI-N-(C-D-F-L-L)	18.4	2.67	>200^c	>200
AIP-III D-N2	I-DN-(C-D-F-L-L)	5.31	0.222	—^{c,d}	23.1
AIP-III D-C3	I-N-(DC-D-F-L-L)	>200	122	>200	>200
AIP-III D-D4	I-N-(C-DD-F-L-L)	77.0	1.15	>200	>200^d
AIP-III D-F5	I-N-(C-D-DF-L-L)	>200	>200	>200	>200
AIP-III D-L6	I-N-(C-D-F-DL-L)	>200	>200	>200	>200
AIP-III D-L7	I-N-(C-D-F-L-DL)	29.3	1.96	—^{e}	47.8
AIP-III I1A	A-N-(C-D-F-L-L)	4.61	1.29	—^{f}	12.5
AIP-III N2A	I-A-(C-D-F-L-L)	1.02	0.137	—^{c,d}	2.64
AIP-III D4A	I-N-(C-A-F-L-L)	0.0820	0.0596	0.163	0.106
AIP-III F5A	I-N-(C-D-A-L-L)	>200	44.7	>200	>200
AIP-III L6A	I-N-(C-D-F-A-L)	>200	>200	>200	>200
AIP-III L7A	I-N-(C-D-F-L-A)	>200	>200	>200	>200
AIP-I^g	Y-S-T-(C-D-F-I-M)	--	3.34	6.12	189
AIP-II^g	G-V-N-A-(C-S-S-L-F)	0.890	--	3.59	1.19
AIP-III^g	I-N-(C-D-F-L-L)	8.07	0.456	--	23.8
AIP-IV^g	Y-S-T-(C-Y-F-I-M)	—^{c,d}	0.0897	1.49	--
tAIP-I D2A^g	Ac-(C-A-F-I-M)	1.45	2.50	0.853	0.361

^{a}See Experimental Section for details of strains and methods. See Supporting Information for plots of antagonism dose response curves. All assays performed in triplicate. -- indicates not tested. ^{b}IC$_{50}$ values determined by testing AIPs over a range of concentrations (200 fM to 10 μM). See Figure 4 and Supporting Information for 95% confidence ranges. ^{c}Dose response curve did not reach 100% inhibition over the concentrations tested. ^{d}Dose response curve upturned at higher concentrations. ^{e}Dose response curve revealed agonism and no antagonism. ^{f}No activity at any concentration tested up to at least 10 μM. ^{g}Control compound.

inhibition trends against AgrC-I, -II, and -IV described above, and support Phe5 and Leu6 as the key hydrophobic endocyclic residues for the modulation of cognate and noncognate AgrC receptors by AIP-III.

Replacement of the AIP-III Cys3 with its D-isomer gave full AgrC-III antagonism only at high concentrations (IC$_{50}$ value > 200 nM; Table 3), suggesting that the stereochemistry of this residue is important for AgrC-III activation. Substitution of Asp4 with D-Asp yielded a similarly weak inhibitor. As discussed above, however, replacing this same residue with alanine (i.e., AIP-III D4A) produced the most potent AgrC-III inhibitor in this series (IC$_{50}$ value = 0.0506 nM). Together, these SAR trends indicate that the side-chain of Asp4 may play a major role in AgrC-III activation but not in initial AIP-III:AgrC-III binding, as AIP-III D4A could strongly inhibit AgrC-III but was incapable of activation.

Throughout these SAR analyses, we made the assumption that the AIP-III analogs were eliciting their activity through directly binding AgrC receptors and outcompeting the native AIP signals. Such a hypothesis is reasonable in view of the close structural similarity of these mutants to the native AIP signals and has been made in prior studies of AIP-I and -II analogs.[71] However, to provide further support for this hypothesis, we performed a competition assay between the native AIPs and our most potent AgrC-III inhibitor, AIP-III D4A, using the gfp-reporter strains (see Experimental Section). We observed that the native AIP signals could be added in a dose-dependent manner to completely eliminate AIP-III D4A inhibition and recover gfp production in each of the four S. aureus groups (see Figure S-2). These data serve to support a competitive mechanism by which AIP-III D4A and the related analogs in this study modulate AgrC activity.

S. aureus Hemolysis Assays. Bacterial reporter strains, such as the S. aureus gfp-reporters above, can certainly facilitate the rapid screening of compounds for potential QS modulators.

However, such responses, while informative, may not accurately reflect physiologically relevant QS phenotypes. We therefore sought to develop an additional assay that would permit us to screen our AIP-III analogs for modulation of a physiologically relevant QS phenotype in S. aureus. Previous studies have established that the production of hemolysins is regulated by the agr QS system.[23−25] Therefore, analogs that inhibit the agr system should also block the production of hemolysins in S. aureus, and we reasoned that this outcome could be readily quantitated by hemolysis assays using red blood cells. To this end, we modified a standard bacterial hemolysis assay to a 96-well microtiter plate format to expedite compound screening[72,73] and tested the AIP-III analogs for their ability to inhibit hemolysis by S. aureus. This work represents, to our knowledge, the first application of hemolysis assays for the study of non-native AIPs as QS modulators.

Briefly, we treated wild-type strains of groups-I−IV S. aureus (listed in Table 2) with the AIP-III analogs and evaluated the cultures for hemolysin activity (see Experimental Section for details). Rabbit red blood cells were incubated with peptide-treated bacterial cultures (∼15 min) in a microtiter plate, after which the samples were pelleted by centrifugation. The culture supernatant was then transferred to new plates, and the concentration of free heme (directly correlated with red blood cell lysis) was quantified by measuring absorbance at 420 nm. Similar to the gfp-reporter assays outlined above, we used the native AIPs (I−IV) and the previously reported global inhibitor tAIP-I D2A as key controls in the hemolysis assays (the cyclic dipeptides were omitted as controls due to their low activities in the gfp-reporter assays). Table 4 summarizes the hemolysis assay data for the control peptides and the 13 AIP-III analogs.

With a few minor exceptions, the relative IC$_{50}$ value trends for the controls and AIP analogs in the hemolysis assay were largely identical to those in the gfp-reporter assays, validating our hemolysis assay protocol as a straightforward method for
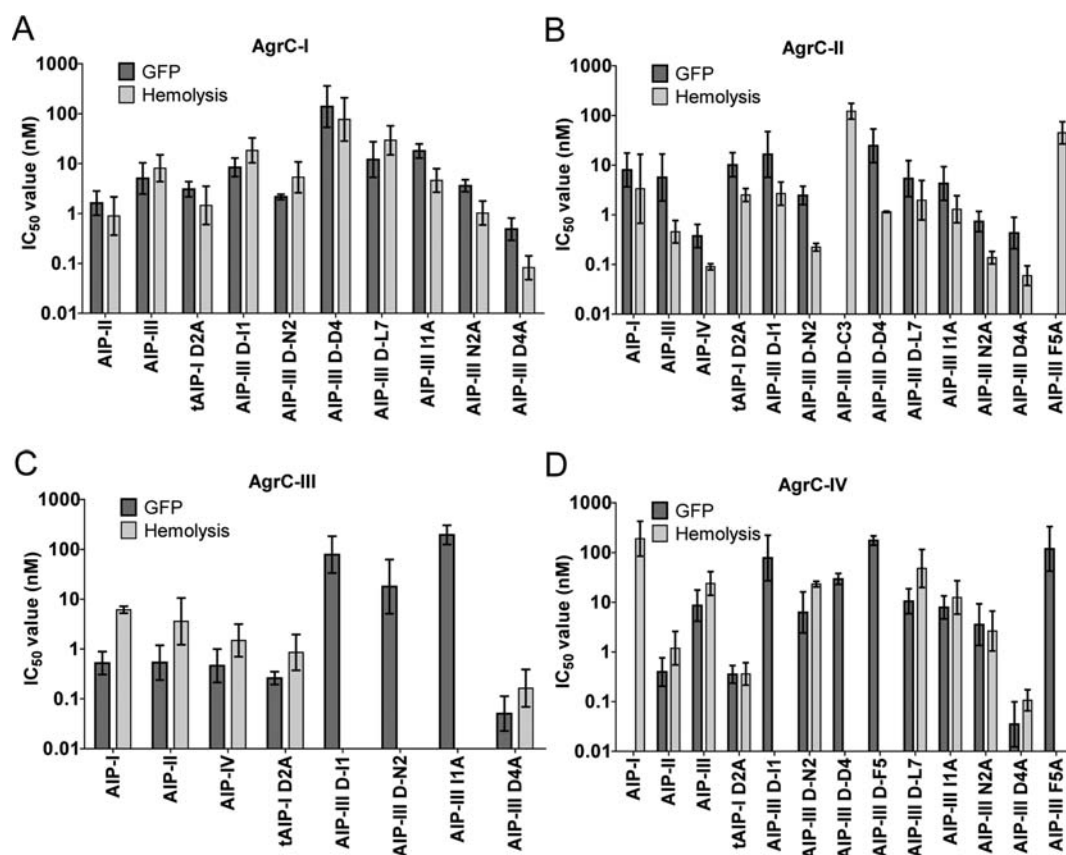
7876

dx.doi.org/10.1021/ja3112115 | J. Am. Chem. Soc. 2013, 135, 7869−7882

Figure 4. IC$_{50}$ values for first-generation AIP-III analogs as determined by the gfp-reporter assay (dark gray) and hemolysis assay (light gray) against: (A) AgrC-I/group-I; (B) AgrC-II/group-II; (C) AgrC-III/group-III; and (D) AgrC-IV/group-IV. Only calculated values (below the 200 nM threshold) are presented. 95% confidence intervals indicated. For a complete listing of data, see Tables 3 and 4.

Table 5. IC$_{50}$ Values of the Second-Generation AIP-III Analogs Against AgrC I–IV Determined Using *S. aureus* Fluorescence Reporter Strains[a]

peptide name	sequence	AgrC-I IC$_{50}$ (nM)[b]	AgrC-II IC$_{50}$ (nM)[b]	AgrC-III IC$_{50}$ (nM)[b]	AgrC-IV IC$_{50}$ (nM)[b]
AIP-III I1A/N2A	A-A-(C-D-F-L-L)	7.40	4.38	2.60	5.41
AIP-III I1A/D4A	A-N-(C-A-F-L-L)	0.328	2.35	0.280	0.101
AIP-III N2A/D4A	I-A-(C-A-F-L-L)	0.331	0.204	0.0657	0.0221
AIP-III I1A/N2A/D4A	A-A-(C-A-F-L-L)	0.304	0.604	0.0734	0.0161
tAIP-III	Ac-(C-D-F-L-L)	26.7	1.53	>200	25.5
tAIP-III D2A	Ac-(C-A-F-L-L)	0.257	0.900	0.329	0.0957
tAIP-III D2A/F3Y	Ac-(C-A-Y-L-L)	0.279	1.15	0.387	0.0306
tAIP-III D2A/F3W	Ac-(C-A-W-L-L)	0.909	1.90	0.509	0.0363
Ac-AIP-III	Ac-I-N-(C-D-F-L-L)	>200	44.3	>200	>200
G-AIP-III	G-I-N-(C-D-F-L-L)	29.9	13.7	>200[c]	104
A-AIP-III	A-I-N-(C-D-F-L-L)	26.1	6.40	27.5[d]	28.5[d]
Y-AIP-III	Y-I-N-(C-D-F-L-L)	8.92	3.75	39.2	78.2[c]
AIP-III D4A[e]	I-N-(C-A-F-L-L)	0.485	0.429	0.0506	0.0349
tAIP-I D2A[e]	Ac-(C-A-F-I-M)	3.06	10.1	0.260	0.353

[a]See Experimental Section for details of reporter strains and methods. See Supporting Information for plots of antagonism dose response curves. All assays performed in triplicate. [b]IC$_{50}$ values determined by testing AIPs over a range of concentrations (200 fM to 10 μM). See Figure 5 and Supporting Information for 95% confidence ranges. [c]Dose response curve did not reach 100% inhibition over the concentrations tested. [d]Inhibition dose response curve upturned at higher concentrations, potentially indicative of partial agonism (see text). [e]Data included for comparison.

the detection and quantification of AgrC modulators in *S. aureus* (Tables 3 and 4; see Figures 4 and S-3–S-6 for a data overlay).[74] The most potent AgrC inhibitors identified in the gfp-reporter assays were capable of completely inhibiting hemolysis in the *S. aureus* strains at nanomolar concentrations or lower. For example, the global *S. aureus* QS inhibitor identified in the gfp-reporter assay, AIP-III D4A, inhibited

hemolysis in all four groups at subnanomolar concentrations (IC$_{50}$ value < 0.2 nM). This peptide was 3-fold more active than the previously reported global inhibitor, tAIP-I D2A, in the hemolysis assay in the group-IV strain; more strikingly, it was 18-fold and >40-fold more active in the group-I and -II strains, respectively (Table 4). These data are significant, as they indicate that AIP-III D4A and related analogs are capable

Table 6. IC$_{50}$ Values of Selected Second-Generation AIP-III Analogs for Inhibition of Hemolysis by Group-I–IV *S. aureus* Strains[a]

peptide name	sequence	group-I IC$_{50}$ (nM)[b]	group-II IC$_{50}$ (nM)[b]	group-III IC$_{50}$ (nM)[b]	group-IVIC$_{50}$ (nM)[b]
AIP-III I1A/D4A	A-N-(C-A-F-L-L)	0.0103	0.793	0.551	0.284
AIP-III N2A/D4A	I-A-(C-A-F-L-L)	0.0362	0.0661	0.216	0.122
AIP-III I1A/N2A/D4A	A-A-(C-A-F-L-L)	0.0411	0.0606	0.243	0.140
tAIP-III D2A	Ac-(C-A-F-L-L)	0.332	0.711	0.197	0.306
tAIP-III D2A/F3Y	Ac-(C-A-Y-L-L)	0.279	0.204	0.265	0.134
tAIP-III D2A/F3W	Ac-(C-A-W-L-L)	0.468	0.126	1.08	0.194

[a]See Experimental Section for details of strains and methods. See Supporting Information for plots of antagonism dose response curves. All assays performed in triplicate. [b]IC$_{50}$ values determined by testing AIPs over a range of concentrations (200 fM to 10 μM). See Figure 5 and Supporting Information for 95% confidence ranges.

of blocking an important QS phenotype directly linked to virulence in wild-type *S. aureus* strains. We later examined their activity against a second virulence phenotype in *S. aureus*, TSST-1 production, which is of particular relevance in the context of AIP-III (Figure 1A). We return to the results of these experiments below.

Second-Generation AIP-III Analogs. We next designed and synthesized a second set of AIP-III analogs to further explore the SARs delineated above for the first-generation analogs and to integrate additional results from prior studies of other synthetic AIP analogs. This set included peptides with double and triple alanine mutations, alternate aromatic residues in place of Phe5, and truncated and elongated exocyclic tails (Table 1). As introduced above, previous reports have demonstrated that truncated AIP-I, -II and -IV analogs lacking the exocyclic tail are strong cross-group inhibitors and weak to strong self-inhibitors of AgrC receptors.[56] In addition, an earlier study revealed that elongation of the exocyclic tail of native AIP-III with a Tyr residue yielded a potent AgrC-III inhibitor.[56] Interestingly, this phenomenon was observed only for AIP-III. While the origins of this effect in AIP-III are unknown, we sought to explore such elongated AIP-III analogs further in the context of the present study. The second set of 12 AIP-III analogs was generated according to the solid-phase synthesis methods introduced above and evaluated in the four *S. aureus* gfp-reporter strains for inhibitory activity against AgrCs-I–IV. The results of these assays are shown in Table 5; data for our lead AgrC inhibitor, AIP-III D4A, and the previously reporter inhibitor, tAIP-I D2A, are included for comparison.

The analogs with double and triple alanine mutations (Table 5, rows 1–4) were designed to examine whether simultaneously replacing multiple amino acid residues with alanine would result in an additive effect on compound activity and built on our studies of the first-generation analogs described above. Replacing both exocyclic residues (Ile1 and Asn2) in AIP-III with alanine yielded an analog (AIP-III I1A/N2A) with an IC$_{50}$ value between those of the parent single alanine mutants for AgrC-I, -II, and -IV (see Tables 3 and 5). In contrast, AIP-III I1A/N2A was a much more potent inhibitor against AgrC-III (IC$_{50}$ = 2.60 nM) relative to the single alanine mutants (I1A, IC$_{50}$ = 194 nM; N2A = weak agonist). Introducing a D4A mutation along with these exocyclic alanine mutations (Table 5, rows 2–4) yielded analogs with antagonistic activities analogous to the AIP-III D4A parent mutant, regardless of other mutations (within error for all except AIP-III I1A/D4A against AgrC-II, with a < 5-fold change), suggesting that the inclusion of D4A may convert most AIP-III mutants into cross-group AgrC inhibitors.

We next examined four truncated AIP-III derivatives lacking exocyclic tails to explore whether this modification, as shown for AIP-I, -II and -IV,[56] could affect their inhibitory activities against cognate and noncognate AgrC receptors (Table 5, rows 5–8). Such an analysis of the native AIP-III is yet to be reported. In agreement with past data for truncated AIP-I and -IV but in contrast to that for truncated AIP-II,[56] we found that the truncated AIP-III (tAIP-III) was only a weak self-inhibitor. Moreover, we observed no significant activity change between tAIP-III and native AIP-III against AgrC-II and -IV and slightly diminished activity for tAIP-III relative to native AIP-III against AgrC-I (26.7 vs 5.05 nM, respectively). These data suggest that the exocyclic tail of AIP-III does not play a major role in cross-group inhibition. We note, however, that inclusion of the D4A mutation in the truncated AIP-III produced a potent global AgrC inhibitor (termed tAIP-III D2A; IC$_{50}$ value < 1 nM for all groups; note, residue numbering shifted due to truncation), with activity within error of its full-length analog (AIP-III D4A) in AgrC-I, -II, and -IV and only somewhat reduced for group-III (IC$_{50}$ value = 0.329 vs 0.0506 nM, respectively). This truncated AIP-III analog represents a more structurally streamlined, peptide-based AgrC inhibitor and provides an excellent scaffold for future structural optimization.

To explore SARs for the lead inhibitor tAIP-III D2A, we replaced Phe3 with other aromatic amino acids (Tyr or Trp) to determine the role of this residue in inhibitory activity (Table 5). These two analogs (tAIP-III D2A/F3Y and tAIP-III D2A/F3W) displayed similar inhibitory activities in the gfp-reporter assays as the parent analog. These data, along with the alanine scan data above, suggest that bulky, aromatic residues are crucial at the Phe3 (or Phe5) position for AgrC recognition by AIP-III analogs but that the residue identity is insignificant.

We next evaluated four elongated AIP-III analogs with either an acetyl, Gly, Ala, or Tyr extension at the N-terminus of AIP-III (Table 5, rows 9–12). Again, elongation of the exocyclic tail of AIP-III with Tyr was previously reported to yield a potent AgrC-III antagonist.[56] As expected, the tyrosine-extended AIP-III (Y-AIP-III) was a moderate antagonist of AgrC-III in the gfp-reporter assay. In contrast, the acetylated and Gly variants (Ac-AIP-III and G-AIP-III) were largely inactive in AgrC-III, and the alanine-extended AIP (A-AIP-III) was actually a partial agonist of AgrC-III instead. When evaluated for inhibitory activity against the noncognate AgrC receptors, Ac-AIP-III was the least active (>200 nM for group-I and -IV and 44.3 nM for group-II), implying that a free N-terminus is important for recognition. None of the elongated AIP-III analogs showed improved inhibition compared to the parent AIP-III, and G-AIP-III was the least potent elongated analog overall. Interestingly, A-AIP-III, as opposed to Y-AIP-III, displayed
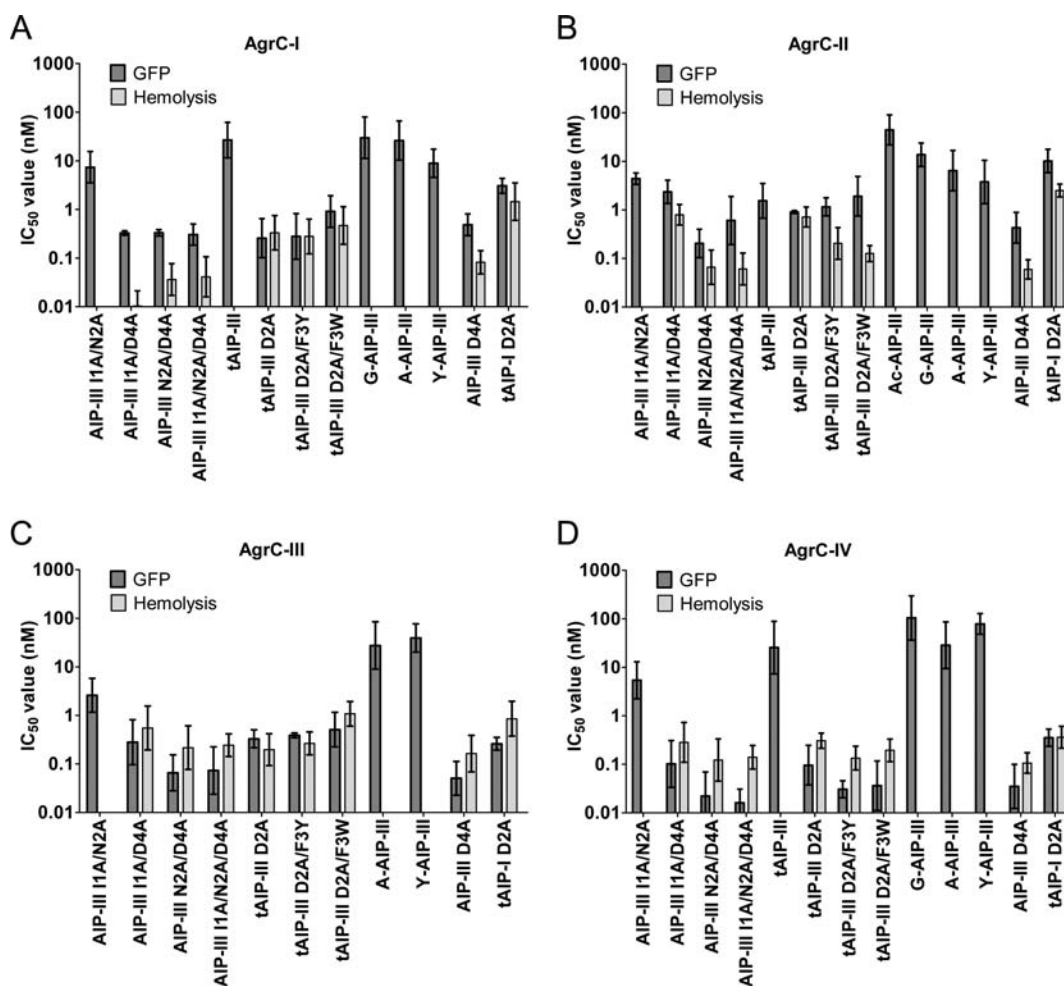
7878

dx.doi.org/10.1021/ja3112115 | *J. Am. Chem. Soc.* 2013, 135, 7869–7882

Figure 5. IC_{50} values for second-generation AIP-III analogs as determined by the gfp-reporter assay (dark gray) and hemolysis assay (light gray) against: (A) AgrC-I/group-I; (B) AgrC-II/group-II; (C) AgrC-III/group-III; and (D) AgrC-IV/group-IV. Only calculated values (below the 200 nM threshold) are presented. In this second generation, only lead compounds (IC_{50} values < 1 nM) were tested in the hemolysis assay. 95% confidence intervals indicated. For a complete listing of data, see Tables 5 and 6.

partial agonism in AgrC-IV, even though Tyr is the first amino acid in this receptor's native AIP sequence (AIP-IV; Figure 1B).

We evaluated the most potent AgrC inhibitors from this second set of AIP-III analogs (IC_{50} values <1 nM) in the *S. aureus* hemolysis assay (Table 6). Analogous to the results for the first-generation analogs, the activity trends for the second-generation analogs in the hemolysis and gfp-reporter assays are largely consistent (see Figure 5 and Figures S-3–S-6 in Supporting Information for a data overlay). However, the hemolysis assay did unmask some variances between certain potent analogs. For example, AIP-III I1A/D4A inhibited hemolysis in group-I at 8-fold lower concentrations than the original AIP-III D4A analog (0.0103 vs 0.0820 nM, respectively), a discrepancy that was not observed in the gfp reporter assays (0.328 vs 0.485 nM, respectively), suggesting that double mutants may enhance the inhibitory activity of AIP-III analogs. We also note that AIP-III D-D4 was a moderate AgrC-IV antagonist in the gfp assay (IC_{50} value = 29.2 nM) but instead displayed partial agonism in the hemolysis assay (IC_{50} value > 200 nM). The cause for the latter discrepancy is unclear at this time. Nevertheless, the overall congruence of the hemolysis and gfp-reporter assay data for both the first- and second-generation AIP analogs in this study provides strong

support for the hemolysis assay as a method to characterize synthetic AgrC modulators.

Attenuation of TSST-1 Production. As highlighted above, this study was motivated in part by our interest in AIP signaling in group-III *S. aureus*, and the production of TSST-1 is a hallmark QS phenotype in this group. Thus, we sought to determine whether the four most potent AgrC inhibitors identified above (AIP-III D4A, tAIP-III D2A, AIP-III N2A/D4A, and AIP-III I1A/N2A/D4A) were capable of reducing the production of TSST-1 in group-III *S. aureus*. We incubated a wild-type group-III *S. aureus* strain (MN8, Table 2) known to produce TSST-1 in the presence of each inhibitor (at 1 and 10 nM) and quantitated toxin production using a standard sandwich-type ELISA assay with a commercially available anti-TSST-1 antibody (see Experimental Section for details). The results of these assays are shown in Figure 6 and demonstrate that all four AIP-III analogs are capable of strongly inhibiting TSST-1 production (by >80%) in this group-III *S. aureus* strain at 10 nM. Moreover, two analogs, AIP-III D4A and tAIP-III D2A, maintained 80% reduction of TSST-1 levels at 1 nM.

These ELISA data are significant, as we are aware of only one other report of small molecules capable of inhibiting TSST-1 production in *S. aureus*—the naturally occurring cyclic
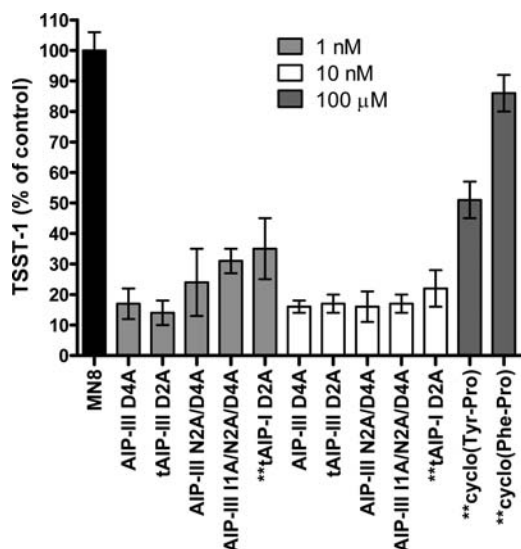
Figure 6. Attenuation of TSST-1 production in wild-type group-III *S. aureus* (MN8) using non-native peptides. Bacteria were either untreated (black bar) or treated with select peptides at 1 nM (light gray bars), 10 nM (white bars), or 100 μM (dark gray bars). TSST-1 concentrations presented as percentage of the TSST-1 concentration in untreated cultures. ** indicates control compound. See text.

dipeptides (cyclo-(Tyr-Pro) and cyclo-(Phe-Pro)) reported by McCormick and co-workers.[34] Bacterial supernatants containing these compounds were shown to reduce TSST-1 production levels by ~80% using an analogous ELISA. The purified cyclic dipeptides, however, were not tested in the ELISA. As we observed these compounds to be largely inactive in the gfp-reporter assays (over the concentration range tested; see above), we reasoned that the pure compounds would be weak inhibitors of TSST-1 production, if at all. We subjected pure samples of cyclo-(Tyr-Pro) and cyclo-(Phe-Pro) to the ELISA protocol and found that 100 μM concentrations were required to reduce TSST-1 production by ~50% or ~15%, respectively (see Figure 6). These data indicate that our AIP-III analogs are at least 1000-fold more potent than the cyclic dipeptides in the ELISA. For an additional comparison, we also evaluated Muir and co-workers' tAIP-I D2A derivative in TSST-1 ELISA. In contrast to the cyclic dipeptides, tAIP-I D2A is a strong inhibitor of the AgrC-III receptor (albeit weaker than the AIP-III analogs; see above). As expected, tAIP-I D2A was capable of inhibiting TSST-1 production by ~80% at 10 nM, yet was less active than AIP-III D4A and tAIP-III D2A at 1 nM (~65% vs ~80%; Figure 6). These AIP-III analogs therefore represent, to our knowledge, the most potent inhibitors of TSST-1 production in *S. aureus* to be reported. Collectively, the results of these ELISA assays, in concert with the hemolysis assay data described above, provide strong support for the use of non-native AIP-III analogs to attenuate clinically relevant QS phenotypes in *S. aureus*.

■ SUMMARY AND CONCLUSIONS

S. aureus utilizes QS to control myriad phenotypes linked to virulence in human infections. This often lethal pathogen uses AIP signals and their corresponding membrane-associated AgrC receptors to mediate QS. Non-native ligands that attenuate AIP signaling in *S. aureus* could be applied as chemical tools to study the role and timing of QS in infection processes. To date, such probe molecules remain limited. In the

current study, we report the design and synthesis of a series of 30 non-native macrocyclic peptides based on the AIP signal used by group-III *S. aureus* for QS, AIP-III. We evaluated the activities of these peptides against the group I−IV AgrC receptors using both fluorescence-based reporter assays and QS phenotypic assays in wild-type *S. aureus* strains. This work revealed a series of new and highly potent, pan-group AgrC inhibitors and represents the first systematic analysis of the SARs defining AIP-III activity in the group I−IV AgrC receptors.

There are several important outcomes of this study. First, SAR analyses of the AIP-III analogs revealed a series of interesting activity trends for AgrC receptor modulation across the four *S. aureus* groups. Our findings both corroborate and extend previous observations regarding the role of the AIP exocyclic residues in AgrC receptor activation as well as the importance of the endocyclic hydrophobic residues for AgrC receptor recognition.[29,52,56] We also demonstrate that, while combining certain mutations in the AIP-III structure led only to modest additive inhibitory effects, inclusion of the D4A mutation consistently converts most AIP-III sequences into potent and global AgrC inhibitors. Specifically, the D4A mutation had this effect in the native AIP-III signal, AIP-III analogs with multiple alanine mutations, truncated AIP-III lacking the exocyclic tail, and truncated sequences with hydrophobic residue mutations. Second, we introduce the use of hemolysis assays as a straightforward, rapid-throughput method to assess a QS phenotype in wild-type *S. aureus* linked to virulence. The similar activity trends observed for the AIP-III analogs in this hemolysis assay compared to those in the gfp-reporter assay serve to validate the utility of hemolysis assays for the study of QS modulators in *S. aureus*.

Third, we extend our studies to examine, for the first time, the effects of AIP analogs on attenuating TSST-1 production in *S. aureus*, a QS phenotype that is particularly pertinent in group-III *S. aureus* infections. Lastly, and perhaps most notably, this study uncovered several global inhibitors of the *S. aureus* agr QS circuit that are active at picomolar concentrations and represent, to our knowledge, the most potent peptide-based AgrC inhibitors reported to date. These results suggest that, relative to the other AIPs, AIP-III provides a superior scaffold for the development of peptide-based AgrC inhibitors. For example, AIP-III D4A surpassed the activity of the known inhibitor, tAIP-I D2A, by 5- to >20-fold in the gfp-reporter assays and by 3- to >40-fold in the hemolysis assays in all four *S. aureus* groups and blocked TSST-1 production in group-III *S. aureus* by over 80% at 1 nM. As such, AIP-III D4A represents a powerful new chemical tool for the study of QS in *S. aureus* in a range of fundamental and applied contexts; its activity in all four groups of *S. aureus* serves to significantly expand its utility. Preliminary assays indicate that the lead AIP-III analogs elicit their inhibitory activity via a competitive mechanism by blocking native AIP-III:AgrC-III binding. Additional biochemical and structural studies are required to characterize their mechanisms of action and will serve to illuminate new avenues for further optimization of their structures to improve their potency and stability. Such studies are ongoing in our laboratory, along with the examination of methods and materials for the controlled release of these agents into environments of relevance for infection control and will be reported in due course.

ASSOCIATED CONTENT

S Supporting Information

Full details of peptide synthesis and characterization, additional bacteriological methods, dose response curves for AIP-III analogs, and overlays of the fluorescence and hemolysis assay data. This material is available free of charge via the Internet at http://pubs.acs.org.

AUTHOR INFORMATION

Corresponding Author

blackwell@chem.wisc.edu

Author Contributions

§These authors contributed equally.

Notes

The authors declare no competing financial interest.

ACKNOWLEDGMENTS

REFERENCES

(1) Ng, W. L.; Bassler, B. L. *Annu. Rev. Genet.* **2009**, *43*, 197−222.

(2) Bassler, B. L.; Losick, R. *Cell* **2006**, *125*, 237−246.

(3) Camilli, A.; Bassler, B. L. *Science* **2006**, *311*, 1113−1116.

(4) Eberhard, A.; Burlingame, A. L.; Eberhard, C.; Kenyon, G. L.; Nealson, K. H.; Oppenheimer, N. J. *Biochemistry* **1981**, *20*, 2444−2449.

(5) Marketon, M. M.; Gronquist, M. R.; Eberhard, A.; Gonzalez, J. E. *J. Bacteriol.* **2002**, *184*, 5686−5695.

(6) Joint, I.; Downie, J. A.; Williams, P. *Philos. Trans. R. Soc., B* **2007**, *362*, 1115−1117.

(7) von Bodman, S. B.; Willey, J. M.; Diggle, S. P. *J. Bacteriol.* **2008**, *190*, 4377−4391.

(8) Boyer, M.; Wisniewski-Dye, F. *FEMS Microbiol. Ecol.* **2009**, *70*, 1−19.

(9) De Kievit, T. R.; Iglewski, B. H. *Infect. Immun.* **2000**, *68*, 4839−4849.

(10) Bjarnsholt, T.; Givskov, M. *Anal. Bioanal. Chem.* **2007**, *387*, 409−414.

(11) Hibbing, M. E.; Fuqua, C.; Parsek, M. R.; Peterson, S. B. *Nat. Rev. Microbiol.* **2010**, *8*, 15−25.

(12) Rasko, D. A.; Sperandio, V. *Nat. Rev. Drug Discovery* **2010**, *9*, 117−128.

(13) Njoroge, J.; Sperandio, V. *EMBO Mol. Med.* **2009**, *1*, 201−210.

(14) Sintim, H. O.; Smith, J. A.; Wang, J. X.; Nakayama, S.; Yan, L. *Future Med. Chem.* **2010**, *2*, 1005−1035.

(15) Wright, G. D. *Curr. Opin. Chem. Biol.* **2003**, *7*, 563−569.

(16) Walsh, C. *Nature* **2000**, *406*, 775−781.

(17) Clatworthy, A. E.; Pierson, E.; Hung, D. T. *Nat. Chem. Biol.* **2007**, *3*, 541−548.

(18) Barczak, A. K.; Hung, D. T. *Curr. Opin. Microbiol.* **2009**, *12*, 490−496.

(19) For an excellent argument against the development of resistance to QS antagonists, see: Swem, L. R.; Swem, D. L.; O'Loughlin, C. T.; Gatmaitan, R.; Zhao, B.; Ulrich, S. M.; Bassler, B. L. *Mol. Cell* **2009**, *35*, 143−153.

(20) Rotun, S. S.; McMath, V.; Schoonmaker, D. J.; Maupin, P. S.; Tenover, F. C.; Hill, B. C.; Ackman, D. M. *Emerging Infect. Dis.* **1999**, *5*, 147−149.

(21) Chambers, H. F.; Deleo, F. R. *Nat. Rev. Microbiol.* **2009**, *7*, 629−641.

(22) Deleo, F. R.; Chambers, H. F. *J. Clin. Invest.* **2009**, *119*, 2464−2474.

(23) Recsei, P.; Kreiswirth, B.; O'Reilly, M.; Schlievert, P.; Gruss, A.; Novick, R. P. *Mol. Gen. Genet.* **1986**, *202*, 58−61.

(24) Pragman, A. A.; Schlievert, P. M. *FEMS Immunol. Med. Microbiol.* **2004**, *42*, 147−154.

(25) George, E. A.; Muir, T. W. *ChemBioChem* **2007**, *8*, 847−855.

(26) Lina, G.; Jarraud, S.; Ji, G. Y.; Greenland, T.; Pedraza, A.; Etienne, J.; Novick, R. P.; Vandenesch, F. *Mol. Microbiol.* **1998**, *28*, 655−662.

(27) Novick, R. P.; Ross, H. F.; Projan, S. J.; Kornblum, J.; Kreiswirth, B.; Moghazeh, S. *EMBO J.* **1993**, *12*, 3967−3975.

(28) Ji, G.; Beavis, R.; Novick, R. P. *Science* **1997**, *276*, 2027−2030.

(29) McDowell, P.; Affas, Z.; Reynolds, C.; Holden, M. T.; Wood, S. J.; Saint, S.; Cockayne, A.; Hill, P. J.; Dodd, C. E.; Bycroft, B. W.; Chan, W. C.; Williams, P. *Mol. Microbiol.* **2001**, *41*, 503−512.

(30) Jarraud, S.; Lyon, G. J.; Figueiredo, A. M.; Gerard, L.; Vandenesch, F.; Etienne, J.; Muir, T. W.; Novick, R. P. *J. Bacteriol.* **2000**, *182*, 6517−6522.

(31) Jarraud, S.; Mougel, C.; Thioulouse, J.; Lina, G.; Meugnier, H.; Forey, F.; Nesme, X.; Etienne, J.; Vandenesch, F. *Infect. Immun.* **2002**, *70*, 631−641.

(32) Holtfreter, S.; Grumann, D.; Schmudde, M.; Nguyen, H. T. T.; Eichler, P.; Strommenger, B.; Kopron, K.; Kolata, J.; Giedrys-Kalemba, S.; Steinmetz, I.; Witte, W.; Broker, B. M. *J. Clin. Microbiol.* **2007**, *45*, 2669−2680.

(33) Limbago, B.; Fosheim, G. E.; Schoonover, V.; Crane, C. E.; Nadle, J.; Petit, S.; Heltzel, D.; Ray, S. M.; Harrison, L. H.; Lynfield, R.; Dumyati, G.; Townes, J. M.; Schaffner, W.; Mu, Y.; Fridkin, S. K. *J. Clin. Microbiol.* **2009**, *47*, 1344−1351.

(34) Li, J. R.; Wang, W. L.; Xu, S. X.; Magarvey, N. A.; McCormick, J. K. *Proc. Natl. Acad. Sci. U.S.A.* **2011**, *108*, 3360−3365.

(35) Musser, J. M.; Schlievert, P. M.; Chow, A. W.; Ewan, P.; Kreiswirth, B. N.; Rosdahl, V. T.; Naidu, A. S.; Witte, W.; Selander, R. K. *Proc. Natl. Acad. Sci. U.S.A.* **1990**, *87*, 225−229.

(36) Galloway, W. R. J. D.; Hodgkinson, J. T.; Bowden, S. D.; Welch, M.; Spring, D. R. *Chem. Rev.* **2011**, *111*, 28−67.

(37) Geske, G. D.; O'Neill, J. C.; Blackwell, H. E. *Chem. Soc. Rev.* **2008**, *37*, 1432−1447.

(38) Persson, T.; Givskov, M.; Nielsen, J. *Curr. Med. Chem.* **2005**, *12*, 3103−3115.

(39) Stevens, A. M.; Queneau, Y.; Soulere, L.; von Bodman, S.; Doutheau, A. *Chem. Rev.* **2011**, *111*, 4−27.

(40) Amara, N.; Krom, B. P.; Kaufmann, G. F.; Meijler, M. M. *Chem. Rev.* **2011**, *111*, 195−208.

(41) Tavassoli, A.; Hamilton, A. D.; Spring, D. R. *Chem. Soc. Rev.* **2011**, *40*, 4269−4270.

(42) O' Connor, C. J.; Laraia, L.; Spring, D. R. *Chem. Soc. Rev.* **2011**, *40*, 4332−4345.

(43) Kaufmann, G. F.; Park, J.; Janda, K. D. *Expert Opin. Biol. Ther.* **2008**, *8*, 719−724.

(44) Geske, G. D.; O'Neill, J. C.; Miller, D. M.; Mattmann, M. E.; Blackwell, H. E. *J. Am. Chem. Soc.* **2007**, *129*, 13613−13625.

(45) Geske, G. D.; ONeill, J. C.; Miller, D. M.; Wezeman, R. J.; Mattmann, M. E.; Lin, Q.; Blackwell, H. E. *ChemBioChem* **2008**, *9*, 389−400.

(46) Mattmann, M. E.; Blackwell, H. E. *J. Org. Chem.* **2010**, *75*, 6737−6746.

(47) Palmer, A. G.; Streng, E.; Blackwell, H. E. *ACS Chem. Biol.* **2011**, *6*, 1348−1356.

(48) Stacy, D. M.; Welsh, M. A.; Rather, P. N.; Blackwell, H. E. *ACS Chem. Biol.* **2012**, *7*, 1719−1728.

(49) Gordon, C. P.; Williams, P.; Chan, W. C. *J. Med. Chem.* **2013**, *56*, 1389−1404.

(50) Park, J.; Jagasia, R.; Kaufmann, G. F.; Mathison, J. C.; Ruiz, D. I.; Moss, J. A.; Meijler, M. M.; Ulevitch, R. J.; Janda, K. D. *Chem. Biol.* **2007**, *14*, 1119−1127.

7881

dx.doi.org/10.1021/ja3112115 | *J. Am. Chem. Soc.* 2013, 135, 7869−7882

(51) Kirchdoerfer, R. N.; Garner, A. L.; Flack, C. E.; Mee, J. M.; Horswill, A. R.; Janda, K. D.; Kaufmann, G. F.; Wilson, I. A. *J. Biol. Chem.* **2011**, *286*, 17351−17358.

(52) Mayville, P.; Ji, G.; Beavis, R.; Yang, H.; Goger, M.; Novick, R. P.; Muir, T. W. *Proc. Natl. Acad. Sci. U.S.A.* **1999**, *96*, 1218−1223.

(53) Lyon, G. J.; Mayville, P.; Muir, T. W.; Novick, R. P. *Proc. Natl. Acad. Sci. U.S.A.* **2000**, *97*, 13330−13335.

(54) Wright, J. S.; Jin, R.; Novick, R. P. *Proc. Natl. Acad. Sci. U.S.A.* **2005**, *102*, 1691−1696.

(55) Fleming, V.; Feil, E.; Sewell, A. K.; Day, N.; Buckling, A.; Massey, R. C. *J. Bacteriol.* **2006**, *188*, 7686−7688.

(56) Lyon, G. J.; Wright, J. S.; Muir, T. W.; Novick, R. P. *Biochemistry* **2002**, *41*, 10095−10104.

(57) Scott, R. J.; Lian, L. Y.; Muharram, S. H.; Cockayne, A.; Wood, S. J.; Bycroft, B. W.; Williams, P.; Chan, W. C. *Bioorg. Med. Chem. Lett.* **2003**, *13*, 2449−2453.

(58) George, E. A.; Novick, R. P.; Muir, T. W. *J. Am. Chem. Soc.* **2008**, *130*, 4914−4924.

(59) Fowler, S. A.; Stacy, D. M.; Blackwell, H. E. *Org. Lett.* **2008**, *10*, 2329−2332.

(60) Chan, W. C.; Coyle, B. J.; Williams, P. *J. Med. Chem.* **2004**, *47*, 4633−4641.

(61) Lyon, G. J.; Novick, R. P. *Peptides* **2004**, *25*, 1389−1403.

(62) Thoendel, M.; Kavanaugh, J. S.; Flack, C. E.; Horswill, A. R. *Chem. Rev.* **2011**, *111*, 117−151.

(63) Gorske, B. C.; Blackwell, H. E. *Org. Biomol. Chem.* **2006**, *4*, 1441−1445.

(64) Campbell, J.; Lin, Q.; Geske, G. D.; Blackwell, H. E. *ACS Chem. Biol.* **2009**, *4*, 1051−1059.

(65) Malone, C. L.; Boles, B. R.; Horswill, A. R. *Appl. Environ. Microbiol.* **2007**, *73*, 6036−6044.

(66) Schlievert, P. M.; Blomster, D. A. *J. Infect. Dis.* **1983**, *147*, 236−242.

(67) Otto, M.; Echner, H.; Voelter, W.; Gotz, F. *Infect. Immun.* **2001**, *69*, 1957−1960.

(68) Sewing, A.; Hilvert, D. *Angew. Chem., Int. Ed.* **2001**, *40*, 3395−3396.

(69) Swinnen, D.; Hilvert, D. *Org. Lett.* **2000**, *2*, 2439−2442.

(70) Dawson, P. E.; Muir, T. W.; Clark-Lewis, I.; Kent, S. B. H. *Science* **1994**, *266*, 776−779.

(71) Lyon, G. J.; Wright, J. S.; Christopoulos, A.; Novick, R. P.; Muir, T. W. *J. Biol. Chem.* **2002**, *277*, 6247−6253.

(72) Blevins, J. S.; Beenken, K. E.; Elasri, M. O.; Hurlburt, B. K.; Smeltzer, M. S. *Infect. Immun.* **2002**, *70*, 470−480.

(73) Lopes, M. D.; Teixeira, L. M. *Rev. Microbiol.* **1992**, *23*, 59−65.

(74) We note that the two sets of assay data came from different bacterial strains (Table 2), and thus strain-to-strain variations could account for the slight deviations observed.